Quaternary Geochronology 76 (2023) 101443

Contents lists available at ScienceDirect

Quaternary Geochronology

journal homepage: www.elsevier.com/locate/quageo

High-resolution ~55 ka paleomagnetic record of Biển Hồ maar lake sediment from Vietnam in relation to detailed ^{14}C and ^{137}Cs geochronologies

Antti E.K. Ojala [a,*], Hướng Nguyễn-Văn [b,**], Ingmar Unkel [c], Dương Nguyễn-Thùy [b], Thái Nguyễn-Đình [b], Quốc Đỗ-Trọng [b], Chunqing Sun [d], Peter E. Sauer [e], Arndt Schimmelmann [e]

[a] Department of Geography and Geology, University of Turku, Turku FI, 20014, Finland
[b] VNU University of Science, Vietnam National University, Hanoi, 334 Nguyễn Trãi Street, Thanh Xuân District, Hà Nội, Viet Nam
[c] Institute of Geography, Heidelberg University, Im Neuenheimer Feld 348, D-69120, Heidelberg, Germany
[d] Institute of Geology and Geophysics, Chinese Academy of Sciences, 19, Beituchengxilu, Chaoyang, Beijing, 100029, China
[e] Indiana University, Department of Earth and Atmospheric Sciences, 1001 East 10th Street, Bloomington, IN, 47405-1405, USA

ARTICLE INFO

Keywords:
Late Pleistocene
Holocene
Southeast Asia
Lake sediment
Paleomagnetic dating
Radiocarbon dating

ABSTRACT

Vietnam's Central Highlands in Pleiku feature numerous volcanic craters (i.e. maars) formed over 0.2 Ma ago that contain continuous high-resolution lacustrine sediment records extending from the Late Pleistocene through the Holocene. Their evolution and sedimentary proxies are potentially powerful archives for interpretation of East-Asian monsoon variability across Vietnam, as well as for local to regional changes in landcover. The focus of this study is to develop a reliable chronology for the Biển Hồ 25-m-long lake sediment sequence in Vietnam's Central Highlands. We present a combined sediment chronology extending back to 55 ka cal BP that is based on ^{137}Cs surface sediment chronology, paleomagnetic dating, and 47 ^{14}C dates distributed evenly throughout the sequence. Based on sedimentary facies analysis and a smooth age-depth model based on ^{137}Cs and ^{14}C data, we infer a long-term stable rate of sedimentation in Biển Hồ lake without unconformities or erosional hiatuses, except for the uppermost section (ca. 100 years) where human activities increase the rate of sedimentation significantly. The Biển Hồ sequence thus provides a complete and uninterrupted record of the lake's depositional history. The present contribution is a geochronologic opening salvo for future contributions from Biển Hồ lake featuring multi-disciplinary evidence for longer-term paleoclimate and environmental changes.

1. Introduction

Past climate and environmental changes recorded in lake sediments can be reconstructed by proxies such as micro- and macrofossils, geochemical components and isotopes, and physical variables, such as mineral magnetic parameters (Thompson and Oldfield, 1986; Smol, 2008). For any paleoclimatic record, it is crucial to establish a reliable chronology for the respective sediment sequence, which connects different sediment depths to their ages *via* a numerical age-depth model (e.g., Blaauw and Christen, 2011). Age-depth models can be constructed in various ways depending on the available results from dating methods and their potential error estimates (Blaauw, 2010; Blaauw and Christen, 2011; Blaauw et al., 2018). In the best case, independently determined ages are cross-checked by multiple methods, for example by using annual increments (varves), or by characteristic sedimentological time markers of historical events such as flood deposits or tephra layers in the sediment succession (e.g., Lowe, 2011; Zolitschka et al., 2015).

Radiocarbon (^{14}C) dating is perhaps the most widely used dating technique for lake sediments containing organic matter. Due to multiple factors influencing the natural content of ^{14}C in an organic sample, a calibration of the ^{14}C measurements is necessary to convert them to calendar dates using internationally ratified calibration curves. The

* Corresponding author.
** Corresponding author.VNU University of Science, Vietnam National University, Hanoi, Viet Nam.
E-mail addresses: antti.e.ojala@utu.fi (A.E.K. Ojala), huongtectonics@vnu.edu.vn (H. Nguyễn-Văn), ingmar.unkel@uni-heidelberg.de (I. Unkel), duongnt_minerals@vnu.edu.vn (D. Nguyễn-Thùy), thai.nd@vnu.edu.vn (T. Nguyễn-Đình), quocdotrong@vnu.edu.vn (Q. Đỗ-Trọng), suncq@mail.iggcas.ac.cn (C. Sun), pesauer@indiana.edu (P.E. Sauer).

https://doi.org/10.1016/j.quageo.2023.101443
Received 10 January 2023; Received in revised form 30 May 2023; Accepted 30 May 2023
Available online 3 June 2023
1871-1014/© 2023 The Authors. Published by Elsevier B.V. This is an open access article under the CC BY license (http://creativecommons.org/licenses/by/4.0/).

most recent edition IntCal20 extends 55,000 years into the past (55 ka cal BP), which corresponds to almost the entire dating range of ^{14}C (Reimer et al., 2020). The precision of ^{14}C ages from the 17th century to 1950 CE is strongly limited by the impact of fossil fuel emissions, the so-called Suess effect (e.g., Graven, 2015), which can however be compensated in the 20th century by accessory cesium (^{137}Cs) dating of relatively young sediment (e.g., Appleby, 2008; Foucher et al., 2021). At the other end of the ^{14}C dating range, geomagnetic excursions such as the Laschamp Event around 41 ka ago (Korte et al., 2019) modulated the ^{14}C production in the upper atmosphere and thus challenge the accuracy of ^{14}C dating in certain intervals (Muscheler et al., 2014).

Paleomagnetic dating, on the other hand, uses the spatial and temporal variability of the Earth's magnetic field, which is defined by the amplitude and duration of changes in polarity, direction (declination, inclination), and strength (intensity) of the magnetic field (Thompson and Oldfield, 1986; Jacobs, 1994). Polarity reversals are of high importance in global magnetostratigraphy and typically occur every 100,000–10 million years (Jacobs, 1994). Within the Late Pleistocene, two other elements are involved in changes of Earth's magnetic field, namely (i) the secular variation (SV), which depends on dipole and non-dipole field behavior and varies on decadal to millennial timescales, and (ii) rapid geomagnetic excursions (geomagnetic 'jerks') with a duration of 500 to 5000 years that involve extreme changes of field direction and intensity (Jacobs, 1994; Laj et al., 2004; Snowball et al., 2007). Mineral grains in lacustrine and marine sediment can acquire remanent magnetization during deposition, thus recording variations in the paleomagnetic field referred to as paleosecular variation (PSV). Natural remanent magnetization (NRM) retained in sediment sequences can be measured and used in correlation and geochronological applications (Thompson and Oldfield, 1986; Snowball et al., 2007).

In this study, we combine atmospheric radionuclide (^{137}Cs), radiocarbon (^{14}C), and paleomagnetic dating approaches to generate a comprehensive and well-constrained chronology for a 25-m-long lacustrine sediment sequence from Biển Hồ maar lake in the Central

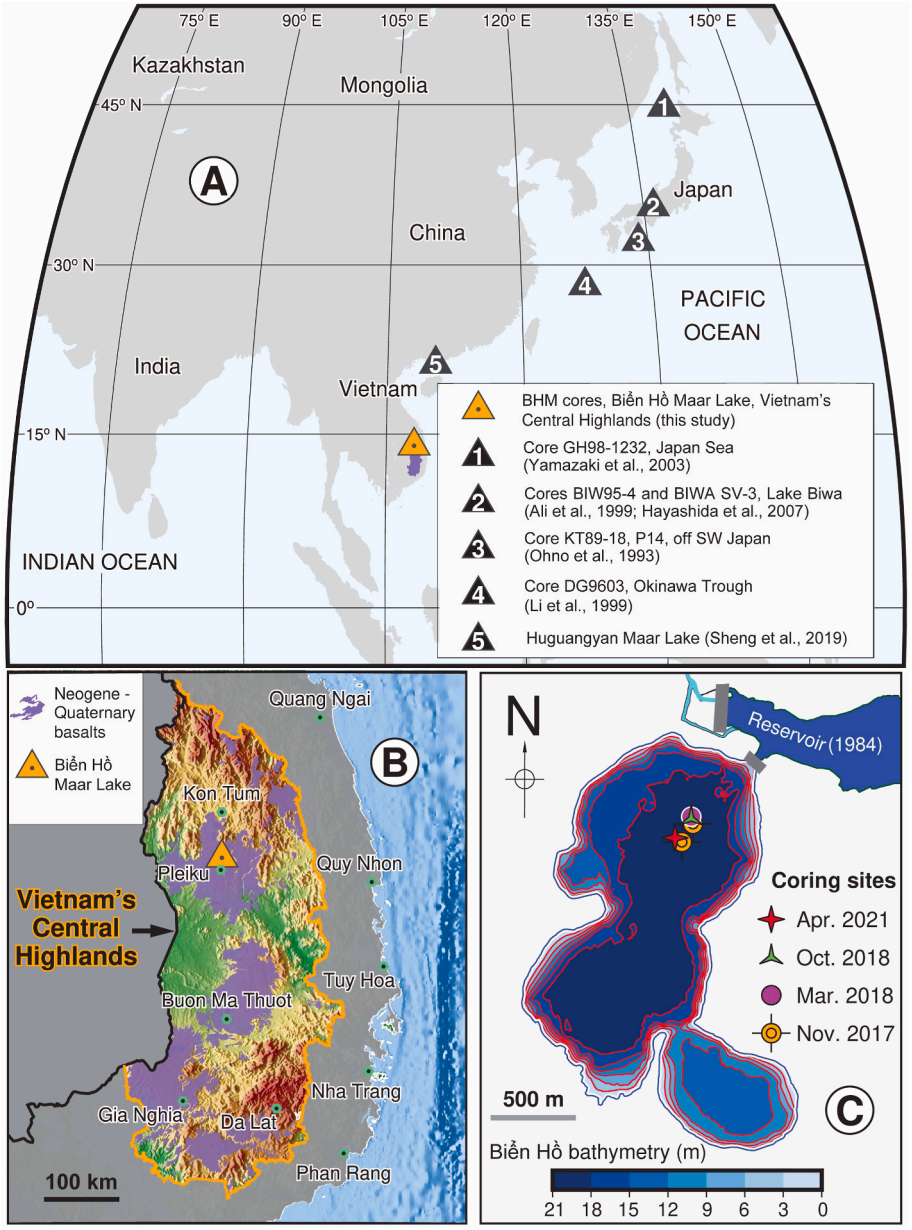

Fig. 1. (A) Location of Biển Hồ maar lake in Asia, along with five sites (identified by black triangles) that are used for paleomagnetic comparison with the present Biển Hồ record. (B) Location of Vietnam's Central Highlands. (C) Biển Hồ coring sites during four campaigns between 2017 and 2021. The bathymetric map is based data from Nguyễn-Văn et al. (2022).

Highlands of Vietnam where seasonal precipitation is strongly linked to the Asian monsoon (Buckley et al., 2014; Nguyễn-Đình et al., 2022; Nguyễn-Văn et al., 2023) (Fig. 1). Without major inflow or outflow, the simple hydrological setting of the formerly closed Biển Hồ maar accumulated a Late Pleistocene to Holocene high-resolution sedimentary record of Asian monsoon variability and has the potential to serve as a regionally important reference archive for paleoenvironmental changes. The uppermost 1.2 m of the Biển Hồ sediment sequence covering the last 70 years documents substantial anthropogenic influence, such as deforestation, crater breaching, and dam and sill construction during the last decades (Nguyễn-Văn et al., 2022). The authors' detailed geographic and historical description of the site laid the groundwork for paleoenvironmental interpretations of Biển Hồ's deeper sedimentary sequence that extends back tens of thousands of years prior to any anthropogenic impact in the catchment of the maar (Nguyễn-Khắc, 2007; Nguyễn-Văn et al., 2022, 2023).

Here, we present a complete record of magnetic PSV based on the Biển Hồ sequence and compare it with existing regional and stacked global PSV reference curves (Laj et al., 2004; Yang et al., 2009). The results of paleomagnetic dating are then compared with the Bayesian age-depth model that is based on 47 accelerator mass-spectrometric (AMS) radiocarbon dates distributed along the 25-m-long profile. We validate and adjust the radiocarbon-based age-depth model over periods of reduced geomagnetic field intensity, such as the Laschamp excursion ~41 ka cal BP (Korte et al., 2019). Our goal is that this intensively radiocarbon-dated Biển Hồ PSV record will provide regional reference curves (inclination and relative paleointensity) on the variability of the geomagnetic field since about 55 ka cal BP. The present study lays essential geochronologic groundwork for on-going studies of the Biển Hồ sediment sequence featuring multi-disciplinary evidence for longer-term paleoclimate and environmental changes.

2. Study site and available cores

Biển Hồ is a maar lake (14.05 °N, 108.00 °E) located in the Pleiku volcanic field close to Pleiku, the capital city of the Gia Lai province in Vietnam. Following their formation more than 200 ka ago, maars in this Cenozoic volcanic field have accumulated sedimentary archives extending from the Holocene far into the Pleistocene (Nguyễn et al., 2013; Nguyễn-Văn et al., 2022).

The lake with a seasonally variable depth of 19–21 m in its central area has a relatively flat bottom topography (Fig. 1). The hydrological catchment is limited to the crater's rim around the basin. There are no natural streams entering or draining out of the basin. The monthly mean air temperature at the study site varies between about 20 and 25 °C. Precipitation is strongly seasonal with a monsoonal July–August peak reaching a monthly total of up to 500 mm. A detailed description of the study site, statistics of modern precipitation and temperature data, and a history of anthropogenic activities around the lake have been compiled by Nguyễn-Văn et al. (2022).

The deepest part of Biển Hồ maar lake has been targeted for the recovery of several sediment cores between 2017 and 2021. Maximum coring depth and quality of retrieved sediment cores increased over the years owing to improvements of a customized piston corer and sampling techniques (Table 1). During the latest coring expedition in April 2021, two parallel and overlapping piston cores were retrieved yielding a sediment sequence of 25 m in length. Individual segments of the two parallel piston cores were taken with a vertical offset relative to each other to produce a continuous overlapping composite record based on downcore variations of whole core logging profiles (gamma density, P-wave velocity, magnetic susceptibility loop, and electrical resistivity), cleaned surfaces of half-cores scanning data (magnetic susceptibility, color profiles and color photographs) (Supplementary Material S1). A more precise correlation was archived based on visual sedimentary features, core facies and, organic matter (Nguyễn-Văn et al., 2023).

All Biển Hồ sediment cores have been split, described and subsampled in laboratories at *Vietnam National University, Hanoi* (VNU), the *National Lacustrine Core Facility/Continental Scientific Drilling Facility* (LacCore/CSD Facility) at the *University of Minnesota*, and at *Indiana University* (IU) in Bloomington, USA. As described by Nguyễn-Văn et al. (2022 and 2023), the cross-correlation of all available core segments along a master depth scale down to the sediment depth of 25 m is based on systematic description and registration of sedimentary facies characteristics, color photographs, loss-on-ignition (LOI), and downcore variations of magnetic susceptibility (Table 1).

Table 1
Available sediment cores with core depths and dating approaches.

Core ID	Coring campaign	Core depth (m)	^{137}Cs dating	^{14}C dating	Paleomagn.
BHM21	April 2021	0–25.1		12 samples	X
BHM8-5-5C		0–0.6	X		
BHM8-2C1-D1	October 2018	0–1.2	X		
BHM8		0–15.3		15 samples	
BHM8	March 2018	0–5.7		7 samples	
BHM7-VN4	November 2017	0.3–1.0	X		
BHM7		0–3.8		13 samples	

3. Methods

The split core sections were described in detail for lithology and sediment structures in the laboratory, followed by logging for magnetic susceptibility with a Bartington MS2E surface-scanning sensor at 1-cm resolution, for water content at 4-cm resolution, and for loss-on-ignition (LOI) at 2-cm resolution. Water content in weight (wt.) % was determined *via* weight loss after freeze drying. LOI (wt. %) was determined by heating dried sediment at 550 °C in a muffle furnace for 4 h (Håkanson and Jansson, 1983).

3.1. Cesium (^{137}Cs) dating

The cesium isotope ^{137}Cs in sediments results entirely from anthropogenic sources and is associated with atmospheric testing of nuclear weapons and accidents in nuclear reactors and reprocessing facilities. The vertical distribution of ^{137}Cs in near-surface sediments has become an essential tool in establishing age models of the most recent past in lacustrine and marine sediment sequences (e.g., Appleby, 2000, 2008; Ojala et al., 2017). In general, measurable amounts of global ^{137}Cs fallout from the atmosphere have occurred since the late 1940s and early 1950s CE, with a first pronounced increase in 1954 CE, followed by a minimum at 1960–61 CE, and a maximum fallout from nuclear weapons testing in 1963 CE. The atmospheric ^{137}Cs fallout then decreased until 1986 CE when a distinct fallout peak resulted from the Chernobyl nuclear accident which predominantly impacted the Northern Hemisphere (e.g., Wright et al., 1999; Appleby, 2000; Klaminder et al., 2012). Another significant atmospheric fallout of ^{137}Cs in the wake of the Fukushima accident in 2011 shows up prominently in some sedimentary records from eastern Asia (Kanai et al., 2013; Ochiai et al., 2013).

Three surface sediment cores from Biển Hồ maar lake were measured for the vertical distribution of ^{137}Cs at 1–2 cm resolution (Table 1) (see also Nguyễn-Văn et al., 2022). All samples were freeze dried and homogenized prior to analysis. The analyses were performed at the Geological Survey of Finland using a fully digital BrightSpec bMCAUSB pulse height analyzer coupled to a well-type NaI(Tl) detector. The activity concentrations of samples were normalized to sample weights. Data were processed using SODICAM quantitative spectrum analysis

software.

3.2. Radiocarbon (^{14}C) dating

We collected 47 samples for ^{14}C dating including macrofossil terrestrial plant fragments and bulk organic carbon in sediment. The samples were taken at average resolution of ~0.5 m from multiple core segments retrieved during the four coring campaigns between 2017 and 2021 (Tables 1 and 2). Single-year plant samples including leaves, grass, and small twig fragments accounted for ~60% of the 47 samples. The most common types of terrestrial plant macrofossils are leaf fragments or single leaves. The leaf specimens selected for ^{14}C dating were well preserved as shown by their large and observable fine-scale structures. Bulk sediment samples for separation of total organic carbon were mainly collected from the 10–25 m depth interval where plant macrofossils were rare or not well preserved. Two paired bulk organic carbon and leaf ages from the same depth intervals (670–671 cm and 2426–2427 cm) were used for initial assessment of reservoir effects in our ^{14}C dating (Table 2).

Pretreatment of samples with accession numbers "*OS-#*" in Table 2 was performed at VNU and IU. Pretreatment included removal of carbonates at low pH, extraction of humic and fulvic acids at elevated pH, removal of siliceous components such as clay minerals with hydrofluoric acid, all with intermittent repeated rinsing in deionized water. The dried residual demineralized particulate organic matter was subsequently combusted at 800 °C off-line to carbon dioxide in the presence of excess copper (II) oxide in evacuated and sealed 9-mm o.d. quartz combustion tubes. Carbon dioxide gas was cryogenically quantified and purified on a vacuum line, sealed in 6-mm o.d. Pyrex® tubes, and submitted to the National Ocean Sciences Accelerator Mass Spectrometry (NOSAMS) facility at Woods Hole Oceanographic Institution for AMS ^{14}C age determination. AMS ^{14}C dating of samples with Accession number "*UBA-#*" (Table 2) was performed at the ^{14}CHRONO Centre for Climate, the Environment and Chronology, Queen's University Belfast, Northern Ireland. These five samples were pretreated by 1 M hydrochloric acid for 1–2 h at 80 °C. Dried organic matter were weighed into pre-combusted quartz tubes with an excess of copper (II) oxide and silver foil, sealed under vacuum, and combusted to carbon dioxide at 850 °C for 8 h. Subsequently, carbon dioxide was converted to graphite in contact with an iron catalyst using the zinc reduction method on a graphitization line (Slota et al., 1987). Graphite was pressed into targets and then transferred to the machine for AMS ^{14}C age determination.

The age-depth model was produced using the R package *rbacon* (Blaauw and Christen, 2011). All dates are reported as Common Era calibrated calendar years (cal CE) with respect to the calibration curve IntCal20 (Reimer et al., 2020).

3.3. Magnetic measurements

For paleo- and mineral-magnetic analyses, the BHM21 sediment core was sampled with discrete 7-cm^3 polystyrene cubes (1.9 × 1.9 × 1.9 cm) that were orientated parallel to the side of the cores and pressed perpendicularly into the wet levelled sediment surface. Altogether, 740 samples were prepared from the 25-m-long sediment sequence of Biển Hồ, with some overlapping of sampling for duplication and quality control.

Low-field magnetic susceptibility (κ) was first measured on each discrete sample cube using a Bartington MS2B sample sensor. Representative samples from seven different depth levels (B-3/6 = 300 cm, B-5/6 = 502.5 cm, B-8/23 = 896.5 cm, B-12/20 = 1298.5 cm, B-18/17 = 1674 cm, B-24/4 = 2104 cm, B-30/17 = 2485.5 cm) were selected for progressive alternating field (AF) demagnetization (0–100 mT peak AF with steps of 5–10 mT) to test the stability of the NRM (Fig. 2). The selection of the test samples was based on sediment lithological characteristics and magnetic susceptibility. Based on NRM demagnetization behavior of the test samples, the remaining samples were measured

Table 2
List of radiocarbon samples taken from Biển Hồ sediment cores. OS-#: Sample treatment was performed at VNU and IU. AMS^{14}C dates were analyzed at NOSAMS, Woods Hole Oceanographic Institution. UBA-#: Sample pretreatment and AMS^{14}C dating were performed in the^{14}CHRONO Centre for Climate, the Environment and Chronology, Queen's University Belfast, Northern Ireland. * = samples for estimation of reservoir effect.

Lab ID	Date ID	^{14}C Age BP	Age +/− 1σ error	Depth (cm)	Dated material	Sample size (μg C)
NOSAMS-151877-50-1	OS-141005	505	20	80	grass	85
NOSAMS-157983-12	OS-146670	430	20	99	leaf	224
NOSAMS-150126-10-1	OS-138914	885	15	113	leaf	789
NOSAMS-150138-11-14	OS-138918	2070	15	135	leaf	738
NOSAMS-150137-11-13	OS-138654	2400	20	158	leaf	521
NOSAMS-150136-11-12	OS-138653	2520	20	175	leaf	487
NOSAMS-150127-13-2	OS-138655	390	15	222	leaf	558
NOSAMS-150128-13-3	OS-138915	3730	20	242	grass	817
NOSAMS-150129-13-4	OS-138649	4050	25	266	leaf	433
NOSAMS-150130-14-5	OS-138650	5550	25	322	leaf	391
NOSAMS-150131-14-6	OS-138916	6310	30	334	grass	838
NOSAMS-150132-15-7	OS-138651	6710	25	339	leaf	319
NOSAMS-150133-15-8	OS-138652	7390	30	365	leaf	182
NOSAMS-150134-15-10	OS-138917	7930	35	395	bark	944
NOSAMS-150135-15-11	OS-138919	7950	35	402	leaf	1034
NOSAMS-151879-55-3	OS-141062	8920	30	445	leaf	800
NOSAMS-151880-55-4	OS-140919	8910	50	450	twig	837
NOSAMS-151881-55-5	OS-140920	9160	50	464	twig	827
NOSAMS-151882-36-6	OS-140921	9920	60	545	leaf	1035
NOSAMS-151883-36-7	OS-141063	9980	35	553	leaf	406
NOSAMS-151884-36-8	OS-141064	10,300	35	567	leaf	800
NOSAMS-157979-1	OS-146659	11,400	50	601	leaf	274

(*continued on next page*)

Table 2 (*continued*)

Lab ID	Date ID	^{14}C Age BP	Age +/− 1σ error	Depth (cm)	Dated material	Sample size (μg C)
NOSAMS-157980-2(*)	OS-146668	13,000	60	670(*)	leaf	228
NOSAMS-157987-18(*)	OS-146663	13,450	60	671(*)	bulk organic carbon	1184
UBA-44232	BH735	14,753	63	756	bulk organic carbon	1200
NOSAMS-157986-17	OS-146662	16,100	80	817	bulk organic carbon	1058
NOSAMS-157985-16	OS-146661	18,400	110	930	bulk organic carbon	1020
NOSAMS-157981-4	OS-146669	17,550	110	942	leaf	110
UBA-44233	BH1022	20,649	116	1054	bulk organic carbon	1200
UBA-44234	BH1121	22,086	141	1144	bulk organic carbon	1200
NOSAMS-157982-7	OS-146660	23,900	220	1227	leaf	427
UBA-44235	BH1310	26,485	231	1328	bulk organic carbon	1200
NOSAMS-174161-1378	OS-162513	27,600	300	1378	leaf	1176
NOSAMS-157988-20	OS-146664	29,200	420	1422	bulk organic carbon	1043
UBA-44236	BH1406	29,411	326	1449	bulk organic carbon	1200
NOSAMS-157984-14	OS-146652	26,900	460	1507	leaf	241
NOSAMS-174162-1523	OS-162514	31,000	450	1523	leaf	528
NOSAMS-174163-1600	OS-162515	35,200	760	1600	bulk organic carbon	1176
NOSAMS-174165-1731	OS-162530	39,100	1200	1731	bulk organic carbon	1020
NOSAMS-174166-1813	OS-162539	41,800	1700	1813	bulk organic carbon	954
NOSAMS-174167-1900	OS-162540	44,000	2300	1900	bulk organic carbon	846
NOSAMS-174168-2000	OS-162541	42,900	2000	2000	bulk organic carbon	953
NOSAMS-174169-2106	OS-162542	47,000	3300	2106	bulk organic carbon	984
NOSAMS-174170-2207	OS-162543	49,700	4600	2207	bulk organic carbon	1008
NOSAMS-174171-2300	OS-162544	48,100	3800	2300	bulk organic carbon	991
NOSAMS-174172-2426(*)	OS-162545	43,600	2100	2426(*)	leaf	828
NOSAMS-174173-2427(*)	OS-162546	46,600	3100	2427(*)	bulk organic carbon	984

without demagnetization and then demagnetized with 20 mT peak AF and re-measured for $NRM_{20\ mT}$. Finally, all samples were subjected to anhysteretic remanent magnetization (ARM), which was induced with a biasing direct field of 0.05 mT superimposed on a peak AF of 100 mT. All ARM samples were demagnetized with 20 mT peak AF and re-measured for $ARM_{20\ mT}$. Progressive AF demagnetization of ARM was done for the same samples and with same steps than with NRM demagnetization. All remanent magnetizations were measured at the Geological Survey of Finland with a 2G Enterprises SRM-755-4 K tri-axial SQUID magnetometer equipped with automated AF demagnetization coils (Ojala et al., 2017).

Inferred relative paleointensity (RPI) was calculated by normalizing the $NRM_{20\ mT}$ to $ARM_{20\ mT}$ according to Levi and Banerjee (1976). The method requires that the magnetic concentration is relatively low and constant throughout the sequence, the carrier of the remanence remains uniform, and pseudo-single domain magnetite is the dominant carrier of the remanence (Levi and Banerjee, 1976; Thompson and Oldfield, 1986; Tauxe, 1993). The magnetic content of the Biển Hồ sequence fulfills these criteria as shown by the present results and according to Nguyễn-Văn et al. (2022).

4. Results

4.1. Sediment characteristics

The Biển Hồ sediment sequence can be roughly divided into two main lithofacies based on sediment characteristics, LOI and mineral magnetic parameters (Fig. 2). These facies are interbedded and exhibit dark olive silty clay and olive-gray diatom-rich silty clay (see Supplementary Material S1) (Nguyễn-Văn et al., 2023). In the upper approximately 6 m, κ varies widely between 60 and 180 SI × 10^{-5} and LOI varies similarly within 10–30 wt %. ARM is clearly associated with magnetic susceptibility, while the ARM/κ ratio increases downcore from the sediment surface to 6 m depth (Fig. 2). The same observation prompted Nguyễn-Văn et al.'s (2022) interpretation that an increased rate of deposition and fluctuations in mineral magnetic signals in the uppermost 1.2 m of near-surface sediment relate to changes in the concentration and grain size of ferrimagnetic minerals, thus providing evidence for intensification of erosion and human induced environmental change. Nguyễn-Văn et al. (2022) further revealed similar magnetic characteristics of Biển Hồ sediment and provenance sediment samples taken around the crater rim, thus suggesting a detrital origin of magnetic minerals from the weathered basaltic catchment.

Below a sediment depth of ~6 m, LOI remains relatively stable around 10 wt %, while κ varies between 20 and 80 SI × 10^{-5}, indicating a relatively homogenous sediment composition. Along the ~20–23 m depth interval, trends of increasing κ and ARM and decreasing ARM/κ indicate a slight increase in concentration of magnetic minerals and a shift toward larger ferrimagnetic grains. However, these changes are not reflected in the sediment water content or LOI. The quality of results for paleomagnetic reconstruction (Thompson and Oldfield, 1986; Snowball et al., 2007) is enhanced by the relatively homogenous distribution of mineral magnetic parameters in the lower lithofacies, despite visually obvious interbedding with more clay-rich (3.5–10 and 20–25 m) and diatom-rich (1–3.5, 10–13 and 15–19 m) intervals.

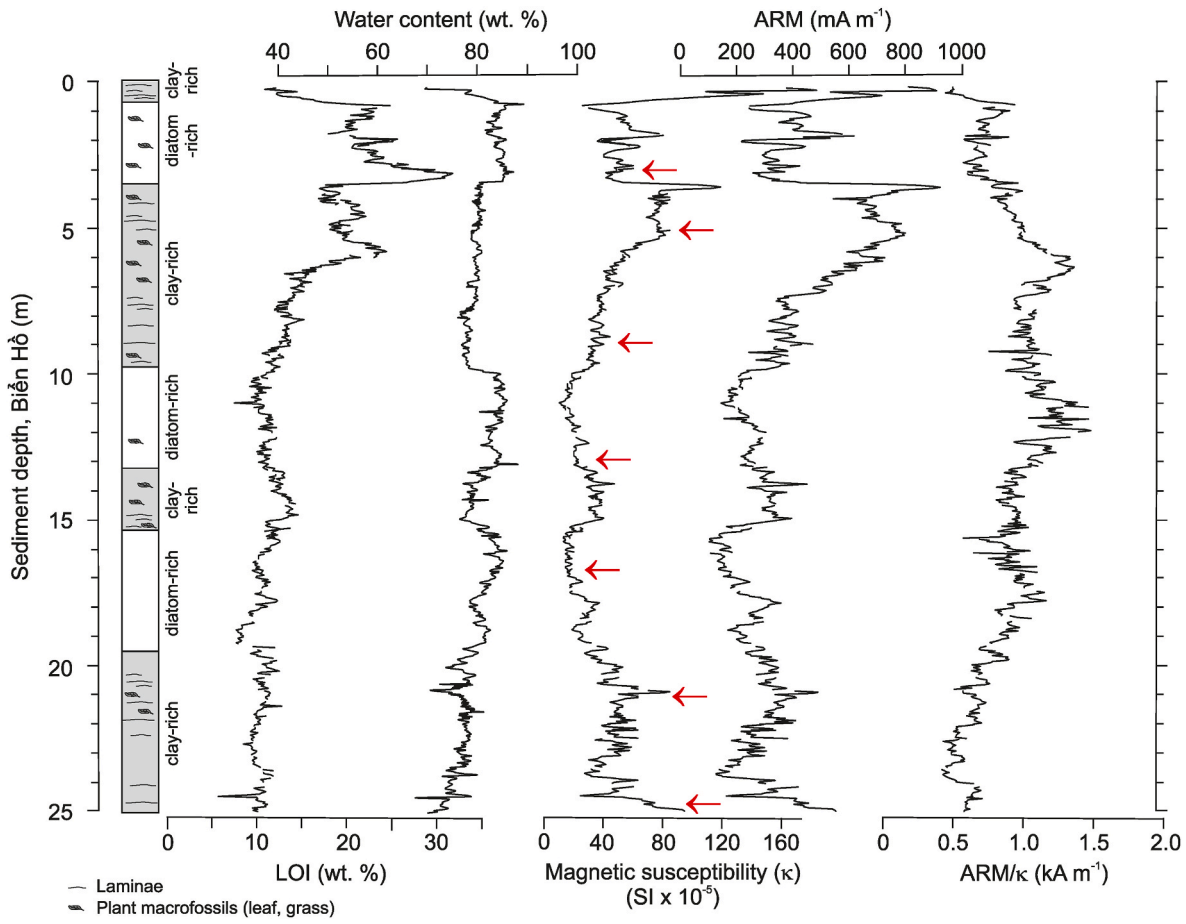

Fig. 2. Physical characteristics of the 25-m-long Biển Hồ sequence (BHM21) with interbedded clay- and diatom-rich sediment facies. Red arrows indicate the origins of test samples selected for constraining NRM stability and core images for the full sediment sequence are shown in Supplementary Material (S1).

4.2. Cesium (^{137}Cs) dating

A stacked record of ^{137}Cs activity from three sediment cores reaching down from the surface is presented in Fig. 3. The profile exhibits low ^{137}Cs abundances in the lower part of the sequence (1.0–1.2 m) and a dramatic increase at ~1 m sediment depth. A clear and well-resolved

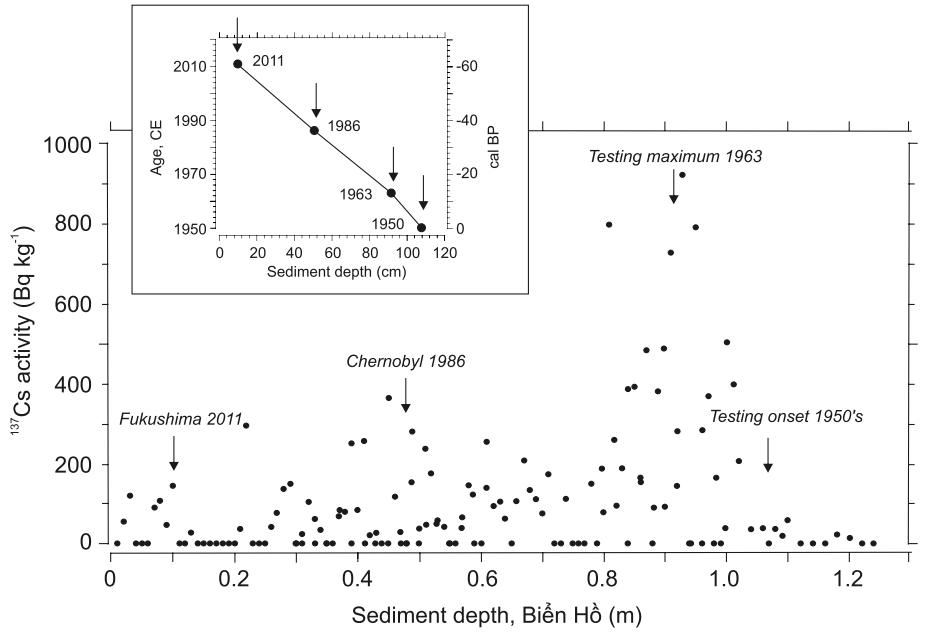

Fig. 3. A stacked record of ^{137}Cs activity in Biển Hồ near-surface sediment (cores BHM8-2C1-D1, BHM8-5-5c, BHM7-VN4) indicates the onset and intermittent maxima from nuclear weapons testing as well as Chernobyl and Fukushima radionuclide fallout and deposition in the lake (updated from Nguyễn-Văn et al., 2022).

peak of 700–920 Bq kg^{-1} of ^{137}Cs activity occurs at 0.8–1.0 m. We consider this dominant feature of the profile as the widely recognized maximum fallout of atmospheric ^{137}Cs related to nuclear weapons testing prior to nuclear test-ban treaties (Appleby, 2000, 2008). Further up-core, an initial decrease of the ^{137}Cs concentration is followed by a renewed increase to 400 Bq kg^{-1} at a depth of 0.4–0.5 m. This increase may be related to atmospheric fallout from the Chernobyl nuclear accident in 1986 CE, although this particular fallout event is often weakly documented in Asia (Bai et al., 2002; Lu, 2004; Ho et al., 2013). The most recent increase in ^{137}Cs activity in the Biển Hồ sequence at ~0.1 m sediment depth relates to the fallout from the Fukushima Dai-ichi nuclear power plant accident in 2011 CE (Long et al., 2012; Kanai et al., 2013; Ochiai et al., 2013). The listed anchor points provide the basis for an age-depth model of the upper part of the Biển Hồ sequence, which agrees well with sedimentological evidence for anthropogenic influence on the rate of sedimentation, as presented and discussed by Nguyễn-Văn et al. (2022).

4.3. Radiocarbon (^{14}C) dating

47 ^{14}C dates covering a sediment sequence of 25 m are an extremely luxurious base for an age-depth-model, especially as more than half of the samples (29 out of 47, Table 2) consist of single-year terrestrial plant material (leaves, small twigs) that are not affected by any water-based reservoir effects. However, the precision of a chronology based purely on ^{14}C dates is limited when covering the entire time period accessible for the ^{14}C method back to 50 ka BP. Calibration tools like *rbacon* use Bayesian statistics, which include *a priori* information such as stratigraphic information of the single dates, which goes beyond the capabilities of the basic calibration with respect to the ^{14}C calibration curve (Fig. 4). Resulting mean age uncertainties of 420 ± 245 years are within the 95% confidence interval during the Holocene, i.e. above 5.6 m depth (Fig. 5). And 2980 ± 1970 years for the Pleistocene part of the sequence, i.e. below 5.6 m depth. Additionally, a standard error of the ^{14}C measurement of only 5% translates into an age uncertainty of ±1500–2500 years before calibration in the period between 30 and 50 ka BP. After calibration, this results in a 95% uncertainty rage of 3000 years or more (Figs. 4–6).

A potential reservoir effect in Biển Hồ lake was investigated by dating two paired ^{14}C samples from bulk organic matter in sediment and leaf samples at two depth intervals of 670–671 cm and 2426–2427 cm (Table 2). When addressing reservoir effects, it is better and more straight forward to refer to ^{14}C concentrations of the samples in percent modern carbon (pmC) instead of the ^{14}C age calculated from these concentrations (Jones et al., 2007). The first pair of samples at 670–671 cm depth (OS-146668 and OS-146663, Table 2) yields concentrations of 19.8 ± 0.148 pmC (leaf) and 18.7 ± 0.139 pmC (bulk organic carbon) respectively, indicating a difference of 1.1 pmC. The second pair of samples at 2426–2427 cm depth (OS-162545 and OS-162546) yields concentrations of 0.44 ± 0.101 pmC (leaf) and 0.30 ± 0.097 pmC (bulk organic carbon), respectively, indicating a difference of only 0.1 pmC. This indicates that the dead (i.e. non-^{14}C) carbon content in the lake may vary over time and thus cannot be addressed as a constant ΔR offset throughout the entire sequence. This may cause potential age offsets of bulk organic carbon samples in the range of the 2-σ age uncertainty of the single-year ^{14}C samples. Here, the combination of ^{14}C dates with information from ^{137}Cs and the paleomagnetic dates helps to improve the age model substantially (see section 4.5).

4.4. Paleomagnetic dating

4.4.1. Demagnetization behavior and stability of natural remanent magnetization (NRM)

The stepwise NRM demagnetization curves for seven test samples are presented in Fig. 7. The median destructive field of test samples varied between 10 and 25 mT. An AF of 100 mT resulted in incomplete, 95–98% demagnetization and indicates (i) the dominance of fine-grained ferrimagnetic magnetite and maghemite (i.e. single-domain SD and pseudo single-domain PSD) as remanence carriers (e.g., King et al., 1982; Thompson, 1986), and (ii) a minor proportion of a 'harder' canted antiferromagnetic mineral(s) carrying robust remanence, such as hematite (King et al., 1982; Thompson, 1986; Thompson and Oldfield, 1986). These results agree with mineral magnetic characteristics of the uppermost 1.2 m of the Biển Hồ sequence presented by Nguyễn-Văn et al. (2022). The presence of ferrimagnetic minerals and a small amount of hematite and goethite in the upper section of the Biển Hồ sequence

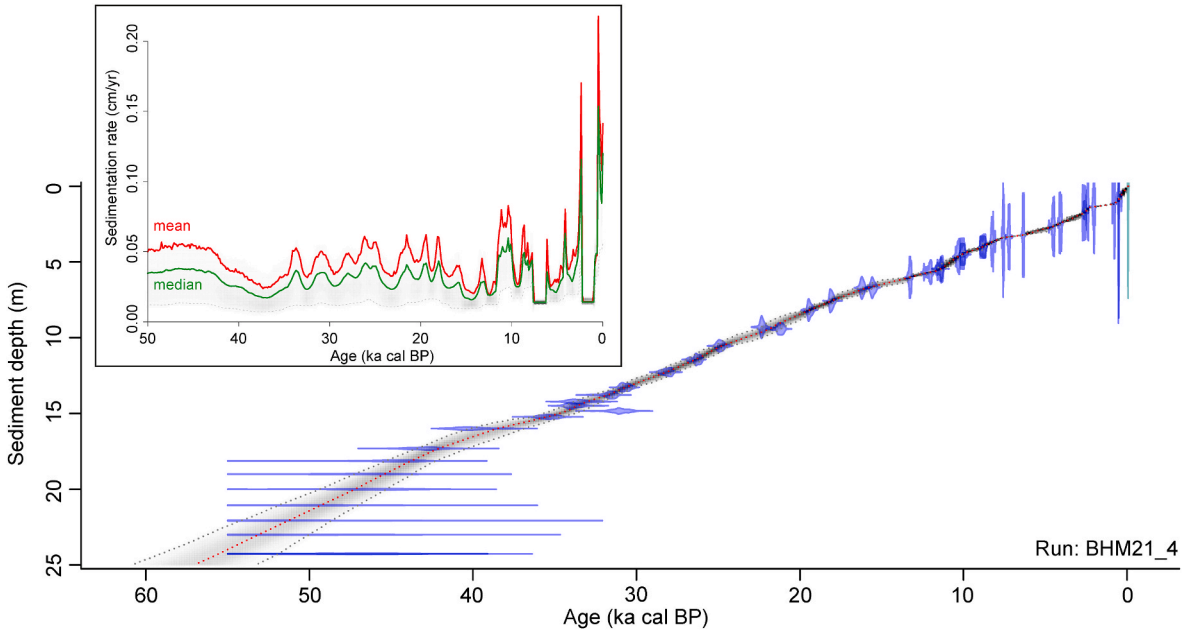

Fig. 4. Bayesian age-depth model of the Biển Hồ maar lake sedimentary sequence without ^{137}Cs and paleomagnetic dates added, created with the R package *rbacon*. The red dashed line represents the weighted mean; gray dashed lines represent minimum and maximum ranges (95% confidence interval). The blue tie bars indicate the ^{14}C age distribution.

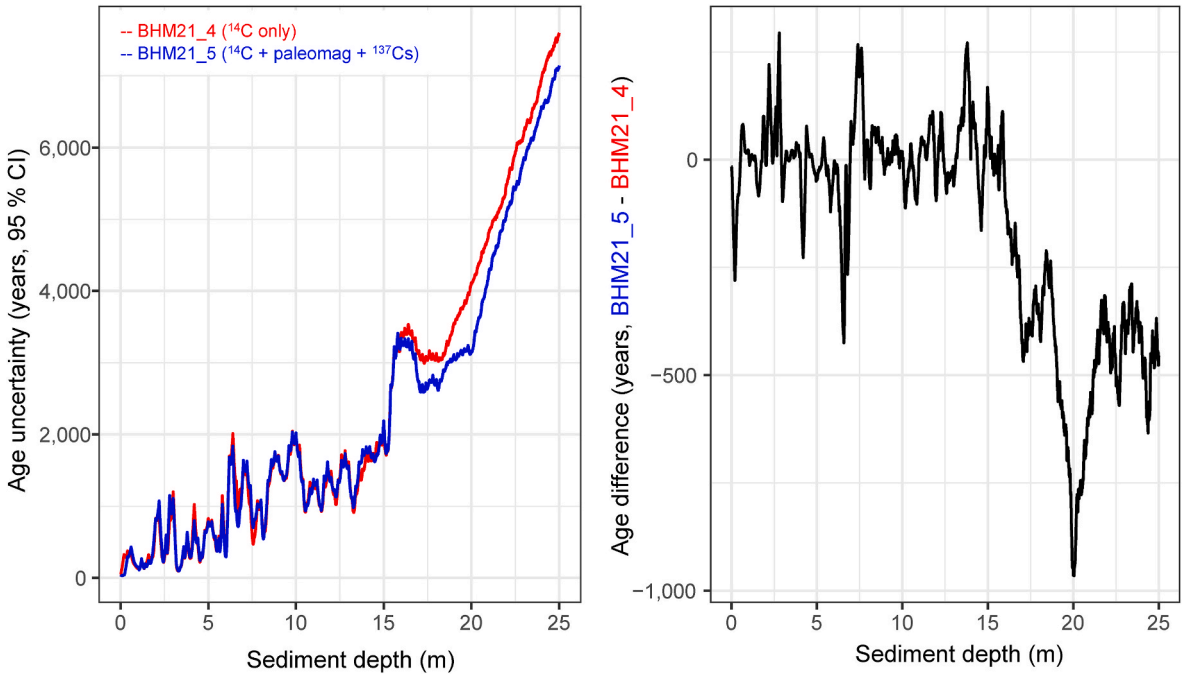

Fig. 5. (Left) Comparison of the ^{14}C-only age-depth-model BHM21_4 (red) and the model BHM21_5 combining ^{14}C with both ^{137}Cs and paleomagnetic dates (blue). With increasing depth (x-axis), the age uncertainty within the 95% confidence interval (y-axis) increases. (Right) Age difference in years of the combined model minus the ^{14}C-only model, indicating the improvement (in negative years) provided by the combined model over the ^{14}C-only model.

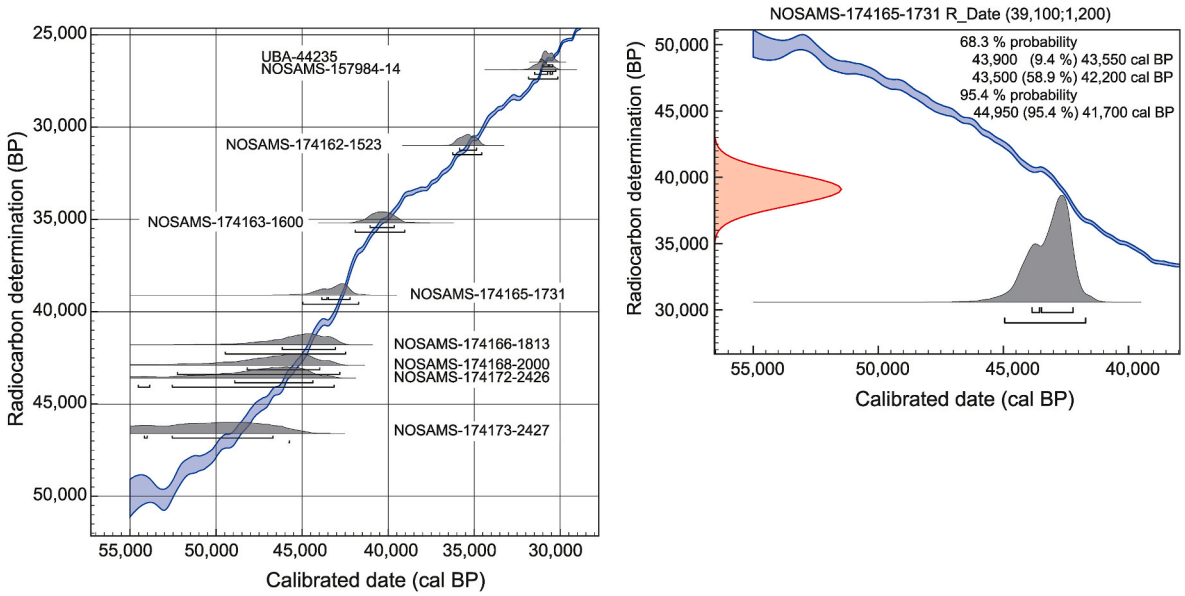

Fig. 6. The left figure presents the lowermost nine ^{14}C dates covering the period of approximately 25–50 ka BP plotted on the calibration curve IntCal20 using OxCal 4.4 (Bronk Ramsey, 2009; Reimer et al., 2020). The gray probability density distribution indicates the 2σ ranges (95.4% probability). The right figure shows how the ^{14}C date NOSAM-174165 located closest to the magnetic Laschamp Event exemplifies the huge 2σ uncertainty range of more than 3000 years (44.95–41.7 ka cal BP) after calibration.

was confirmed *via* XRD analyses (Nguyễn-Văn et al., 2022). Importantly, similar and smooth shapes of demagnetization curves from deeper depth levels presented in Fig. 7 indicate that the magnetic mineral content of the Biển Hồ sediment remains fairly uniform throughout the 25 m long sequence, albeit it is characterized by fluctuations in concentration and grain-size of ferrimagnetic minerals (Nguyễn-Văn et al., 2022).

Orthogonal Zijderveld projections of the seven test samples from different depths of the Biển Hồ sequence (Fig. 2) indicate that two components contribute to the NRM signal, namely (i) a weak and scattered component, and (ii) a strong and stable component that can be considered the primary component of the magnetic direction (Fig. 8). The first component represents viscous remanent magnetization (VRM), which is magnetically softer than the primary component and therefore needs to be removed prior to interpretation of paleosecular variation (PSV) changes in the Biển Hồ sequence during the Late Pleistocene and Holocene. Based on test samples, the VRM was removed in an AF of <15 mT, typically between 5 and 10 mT, which is why all samples were demagnetized at 20 mT ($NRM_{20\ mT}$) during NRM analysis. An

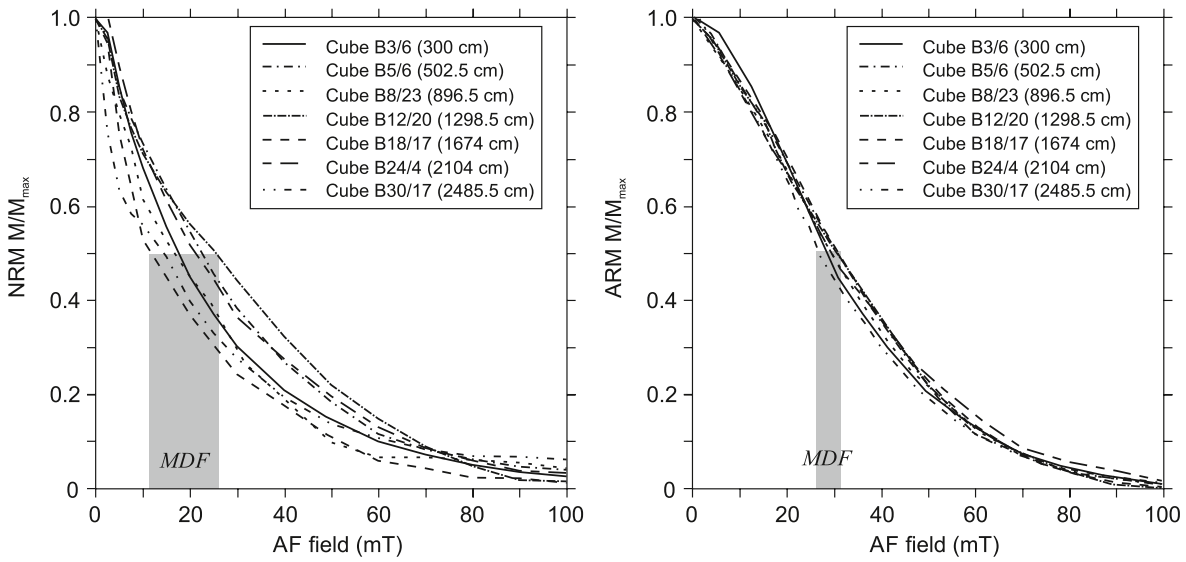

Fig. 7. Stepwise alternating field (AF) demagnetization curves of NRM (on the left) and ARM (on the right) that were calculated for seven test samples from the Biển Hồ sediment sequence indicate typical smooth demagnetization of ferrimagnetic minerals. M/M$_{max}$ is the ratio of intensity left during demagnetizations steps and MDF (median destructive field) is a coercivity indicator that stands for AF required to demagnetize half of the initial remanence. Note that the ARM and NRM demagnetization behavior is very similar between samples and the relative decrease of intensities is similar.

appearance of VRM is often recognized in sediments that contain pseudo-single domain and multi-domain ferrimagnetic grains (e.g., Tivey and Johnson, 1981; Thompson and Oldfield, 1986). This is probably the case with Biển Hồ sediment, although the origin of VRM remains uncertain. VRM could have been introduced during coring or was developed during sample storage or subsampling for paleomagnetic analysis.

The second component of NRM in the Biển Hồ sequence represents a stable primary component and can be considered depositional remanent magnetization (DRM) (Fig. 8). DRM is formed in clastic sediment when fine-grained magnetic particles are deposited on the lake floor in alignment with Earth's prevailing magnetic field during or soon after deposition. Minerals can remain in their preferred magnetic orientation during burial (Thompson and Oldfield, 1986). Orthogonal Zijderveld projections of stepwise AF demagnetization of NRM were calculated for all test samples and are available as part of the Supplementary Material (S2). The present study uses composites of DRM features in the Biển Hồ sequence to independently assign paleomagnetic ages *via* correlation of the directional PSV features and relative paleointensity (RPI) with other global and regional paleomagnetic geochronologic records.

4.4.2. Direction of detrital remanent magnetization (DRM)

Downcore changes in the inclination of DRM in the Biển Hồ sequence are plotted in Fig. 9. The Biển Hồ PSV record expresses distinct patterns and characteristics that can be correlated with marine (Ohno et al., 1993; Li et al., 1999; Yamazaki et al., 2003; Yang et al., 2009) and terrestrial-lacustrine (Ali et al., 1999; Hayashida et al., 2007; Sheng et al., 2019) PSV records from Asia. The downward fluctuating trend of DRM inclination in Biển Hồ is comparable with published DRM reference curves that show positive and negative inclination values with a similar degree of scattering. The reliability of the results presented here is supported by the fact that measured DRM inclination values for Biển Hồ mostly vary within 10–15° on either side of the predicted 15° geoaxial dipole field for Biển Hồ's location.

PSV inclination minima described in other PSV records occur in the Biển Hồ sequence between 2.5 and 12 m depth as inclination minimum features 'a'–'g' (Table 3, Fig. 9). The ages in calendar years BP (cal BP) for these characteristics are based on the well-dated Lake Biwa record (Ali et al., 1999; Hayashida et al., 2007) and range from 4.5 to 29 ka cal BP. For the lower part of the Biển Hồ sequence, the broad PSV inclination lows X1 and X2 are consistent with the characteristics of marine PSV records that extend sufficiently back in time (Ohno et al., 1993; Li et al., 1999), whereas X3 is not seen in other records. The upper features X1 and X2 have been reported from Mono Lake and Laschamp geomagnetic excursions (Korte et al., 2019) (Fig. 9).

Despite efforts to retrieve successive segments of piston cores from Biển Hồ in azimuthal orientation, some measured declination data from individual core segments expressed considerable offsets. We decided against the use of these data because even minor random rotation of individual core segments precluded an accurate representation of PSV declination changes over time.

4.4.3. Relative paleointensity (RPI)

The inferred RPI recorded in the Biển Hồ sequence was compared with the North Atlantic paleointensity stack NAPIS-75 (Laj et al., 2000), the global relative paleointensity stack GLOPIS-75 (Laj et al., 2004), and the paleointensity framework for the South China Sea SCS-PIS (Yang et al., 2009) (Fig. 10). These datasets are known to exhibit similar patterns and provide a globally coherent dating framework for sediments, albeit with some temporal offsets of regional paleointensity (e.g., Yang et al., 2009; Korte et al., 2019). These magnetic chronologies are based on multiple sediment cores independently dated by radiocarbon and tephra chronologies. Anomalous geomagnetic behavior occurred during the Mono Lake – Laschamp interval (~28–45 ka cal BP) with fluctuations of magnetic inclination (see X1–X2 in Fig. 9) (Mankinen and Wenthworth, 2004) and a weak geomagnetic dipole for the well-documented Mono Lake (~33 ka cal BP) and Laschamp (~41 ka cal BP) geomagnetic excursions (e.g., Brown et al., 2018; Korte et al., 2019).

The Mono Lake and Laschamp geomagnetic RPI excursions are also seen in the Biển Hồ sequence with low relative RPI paleointensities at depths of 14.5 and 17 m, respectively (Fig. 10, Table 3). The similarity of these RPI anomalies in the Biển Hồ record with those of the reference curves provide useful anchor points for paleomagnetic dating. In addition, the Biển Hồ RPI record exhibits a maximum at a depth of ~20 m dating to 47 ka cal BP and provides the lowest RPI anchor point in comparison with the GLOPIS-75 and SCS-PIS stacks. Deep ~64.5 ka cal BP RPI minima in the GLOPIS-75 and SCS-PIS stacks are termed the Norwegian-Greenland-Sea excursion and have been detected especially at northern latitudes (e.g., Nowaczyk et al., 2013; Liu et al., 2020), but are not captured in the available Biển Hồ record. This observation is in

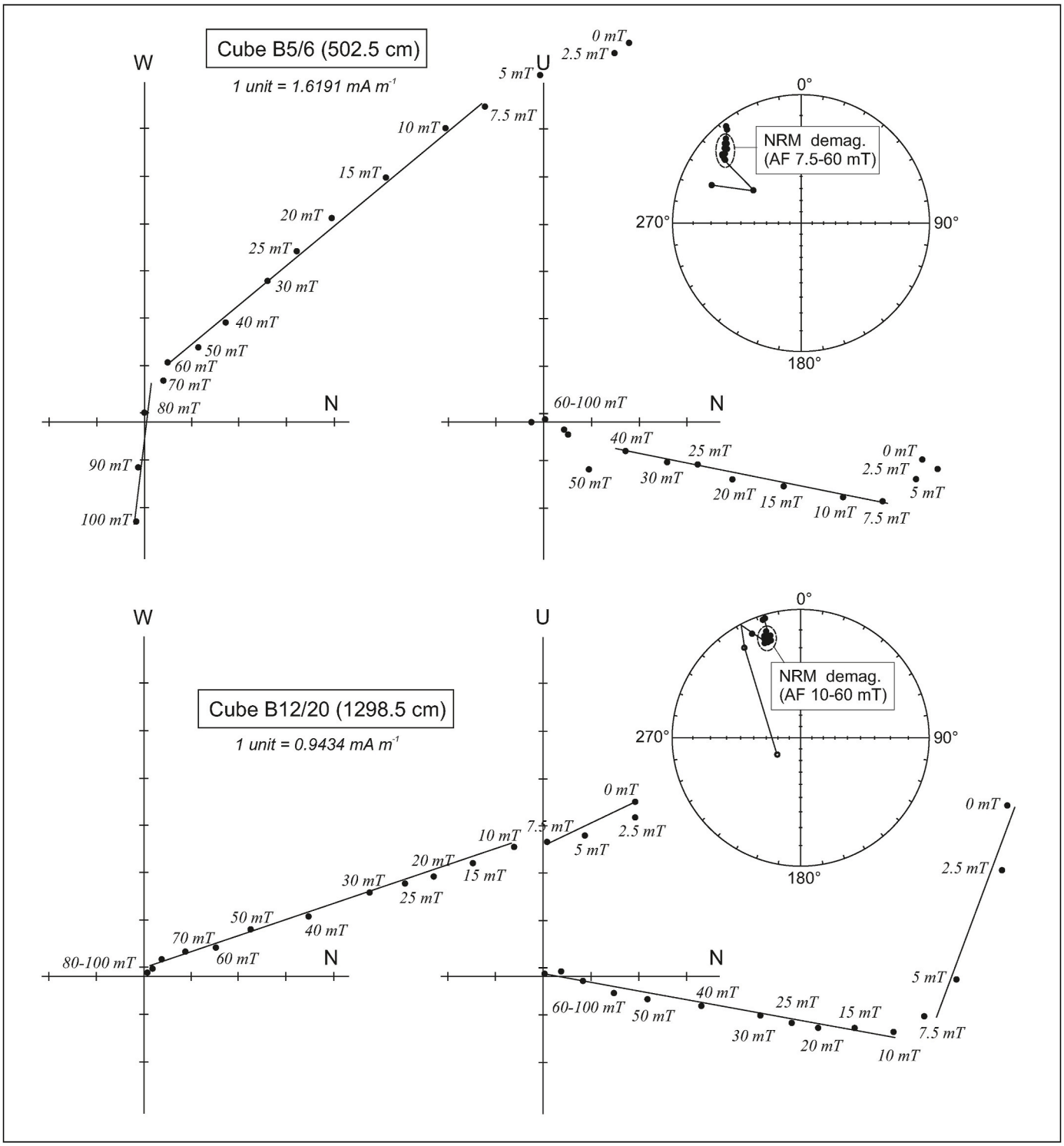

Fig. 8. Orthogonal Zijderveld projections of stepwise AF demagnetization of NRM calculated for two of the selected seven pilot samples from the Biển Hồ sediment sequence indicate an unstable viscous component (0–5 mT for cube B5/6 and 0–7.5 mT for cube B12/20) and a stable primary component of NRM directions (7.5–60 mT for cube B5/6 and 10–60 mT for cube B12/20). Data for all seven test samples are presented as Supplementary Material (S2).

an agreement with the Biển Hồ radiocarbon age-depth model postulating a maximum age of 60.5–53.4 ka BP (median age 56.8 ka BP) for the deepest recovered sediment at a depth of 25 m.

4.5. Combined age-depth model

The paleomagnetic dating of the Biển Hồ sediment sequence is based on matching seven inclination features and three RPI features with available reference points as presented in Figs. 9 and 10. These ten anchor points between 4.5 and 47 ka cal BP (Table 3) were used to assign ages to the respective paleomagnetic sampling depths between 2.5 and 20 m (Fig. 11, Table 3). The relatively smooth and overall quasi-linear appearance of the age-depth curve connecting the anchor points (Fig. 11) illustrates that the average sedimentation rate in Biển Hồ has

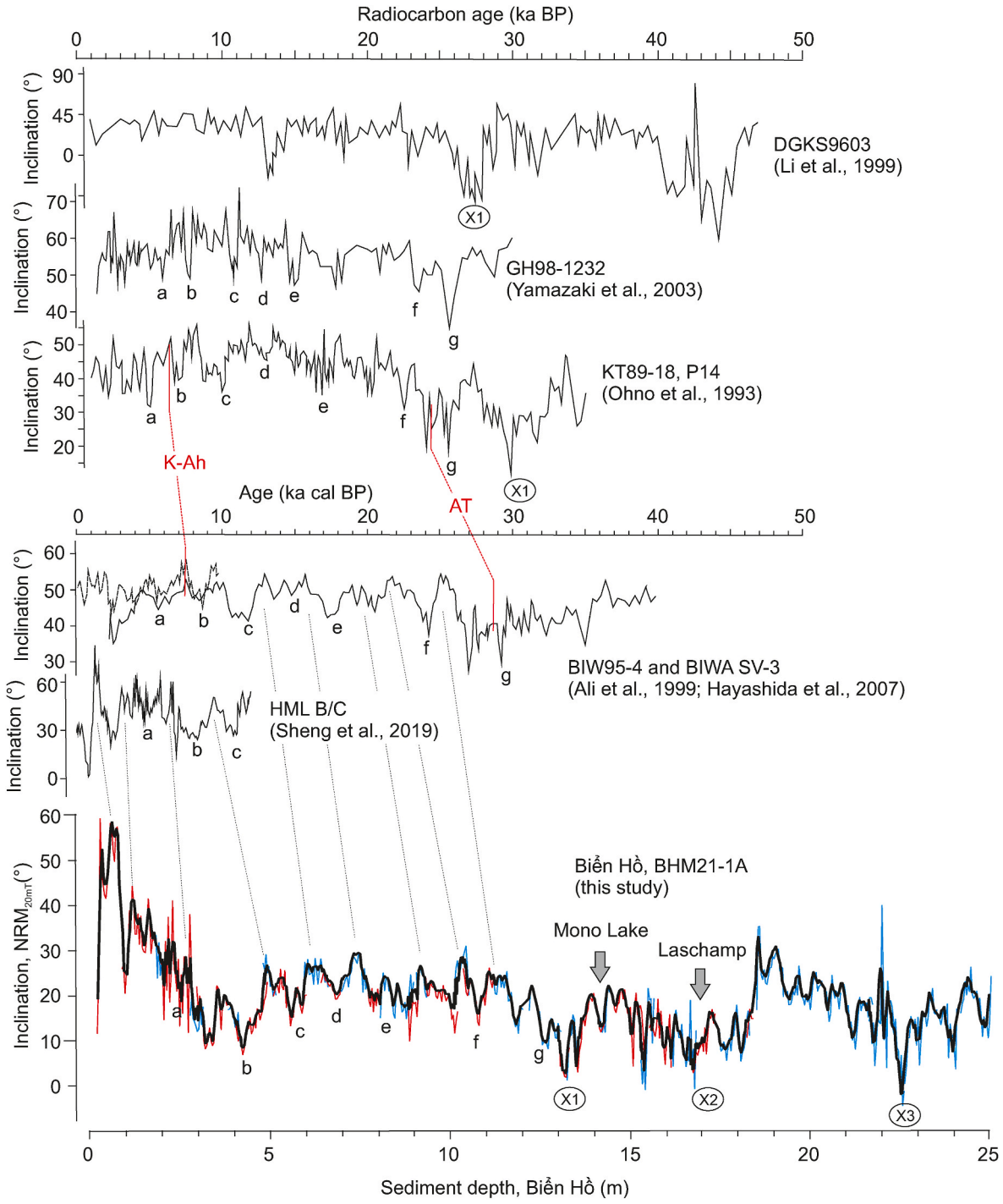

Fig. 9. Variation of PSV inclination based on detrital remanent magnetization (DRM) in the Biển Hồ sequence after AF demagnetization at 20 mT, compared with nearby marine (Ohno et al., 1993; Li et al., 1999; Yamazaki et al., 2003) and terrestrial-lacustrine (Ali et al., 1999; Hayashida et al., 2007; Sheng et al., 2019) PSV records. The naming of intermittent inclination minima with letters 'a' to 'g' is adopted from the given references. X1, X2, and X3 represent broad inclination minima. Dashed lines guide the eye in connecting prominent curve characteristics. K-Ah and AT indicate the occurrence of tephras constrained by Hayashida et al. (2007). Note that the uppermost three comparison curves (Ohno et al., 1993; Li et al., 1999; Yamazaki et al., 2003) are based on uncalibrated ^{14}C dates, whereas the other two (Ali et al., 1999; Hayashida et al., 2007; Sheng et al., 2019) are based on calibrated ^{14}C dates. Blue and red lines in the bottom panel are raw PSV measurements of overlapping cores, whereas the thicker black line is based on 5-point smoothed averages.

remained rather stable at ~0.041 cm per year throughout the entire sequence without recognizable gaps or interruptions.

The ten paleomagnetic anchor points were then integrated in the Bayesian age-depth model in *rbacon* (run BHM21_5, Fig. 12) together with three ^{137}Cs dates, providing additional *a priori* information beyond the 47 ^{14}C dates. To account for dating uncertainties of the paleomagnetic information, an uncertainty range of ±200 years was applied to dates <20 ka, of ±500 years to dates <40 ka, and of ±1000 years to dates >40 ka, respectively. In particular, the Mono Lake and Laschamp geomagnetic excursions fit seamlessly in the radiocarbon age-depth model, which is important because the radiocarbon chronology already exhibits relatively high uncertainty at this age range. At greater

Table 3
Chronology of distinct DRM inclination (INCL min) and RPI features determined from the Biển Hồ sequence. Calendar ages (ka cal BP) are based on Ohno et al. (1993), Ali et al. (1999), Laj et al. (2004), Hayashida et al. (2007), Yang et al. (2009), and Sheng et al. (2019).

Horizon ID	Feature	Sediment depth (m)	Age (ka cal BP)
a	INCL min	2.5	4.5
b	INCL min	4.3	8.5
c	INCL min	5.8	12
d	INCL min	6.8	15
e	INCL min	8.0	18
f	INCL min	10.7	24
g	INCL min	12.5	29
Mono Lake	RPI	14.5	33
Laschamp	RPI	17.0	41
RPI max	RPI	20.0	47

depth and with approaching technical limits of radiocarbon dating, geomagnetic dating becomes increasingly important for Biển Hồ geochronology. In the Pleistocene part of the sequence (older than 11.7 ka cal BP, below 5.6 m depth), the mean age uncertainty decreases to 2780 ± 1780 years within the 95% confidence interval, which is an improvement of 200 years on average compared to the ^{14}C-only model (*rbacon* run BHM21_4, Fig. 4). Around 20 ka cal BP, the improvement compared to the model without paleomagnetic age information is even in the range of 1000 years (Fig. 5).

5. Discussion

Precision and accuracy of paleomagnetic dating are limited mainly by (i) the confidence in the chronology of the reference curve or polarity changes, and (ii) by the spatial and temporal correspondence between the studied sequence and the reference sequence (Thompson and Oldfield, 1986). As observed in the present results, the dominant swings of PSV inclination and relative paleointensity features can be correlated between Biển Hồ data and other east Asian marine and lacustrine PSV records (Figs. 1, 9 and 10), suggesting that directional and intensity patterns are regional in scale and of geomagnetic origin. However, differences in sampling resolution due to sampling frequency and the rate of sedimentation probably varies significantly between sites. Considering the 4-cm sampling resolution of the Biển Hồ sequence, the temporal resolution is approximately 100 years on average, which determines the limits of our paleomagnetic dating precision. However, from previous studies we know that significant and regionally relevant shifts in the direction and strength of Earth's magnetic field during the Late Pleistocene and Holocene exhibit multi-centennial to millennial patterns, rather than decadal swings (e.g., Snowball et al., 2007; Brown et al., 2018; Korte et al., 2019).

The degree of PSV signal smoothing depends to a large extent on the rate of sediment accumulation in the geoarchive under investigation and the sampling intervals at which paleomagnetic measurements are taken. In comparison to other individual and stacked records (see Figs. 9 and 10), the Biển Hồ PSV/RPI record has the highest temporal resolution, thereby securing the potential of PSV and RPI curves to indicate all ranges of typical variability. We assume that the independent reference curve chronologies are accurate. Another potential source of age uncertainty arises from a correlation between the Biển Hồ data and the reference curve, which was done visually and without quantitative correlation methods. To account for that, we applied 2-σ error margins

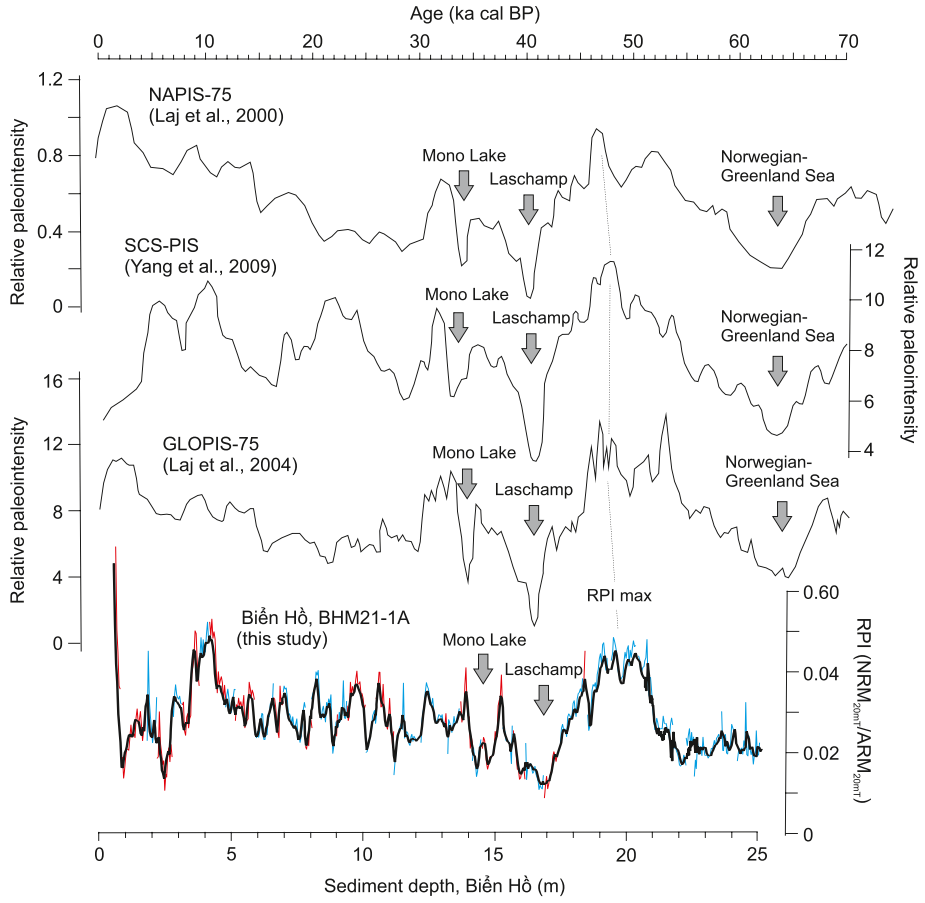

Fig. 10. Correlation of the Biển Hồ RPI record with NAPIS-75 (Laj et al., 2000), SCS-PIS (Yang et al., 2009), and GLOPIS-75 (Laj et al., 2004). The dashed line guides the eye in connecting RPI maxima at ~47 ka cal BP among different curves. Gray arrows point to geomagnetic excursions associated with the Mono Lake (~33 ka cal BP) and Laschamp (~41 ka cal BP) events.

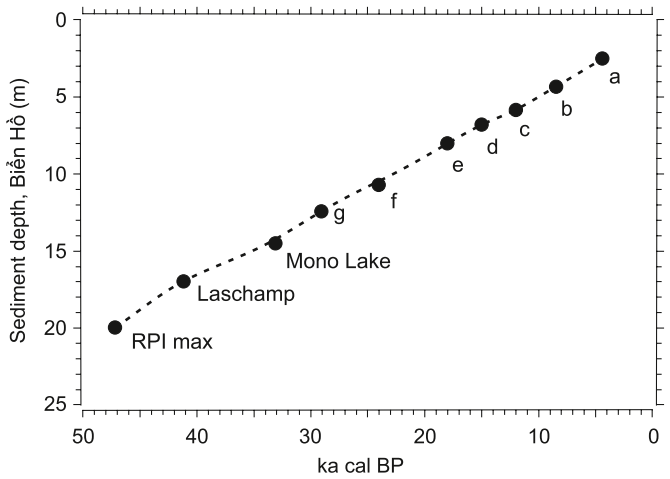

Fig. 11. Paleomagnetic age-depth model for the Biển Hồ sediment sequence based on DRM inclination and RPI features (see Table 3). The dashed line is a fitted polynomial trendline.

between ±200 and 1.000 years when implementing the paleomagnetic dates in the radiocarbon model as outlined above.

Uncertainties of DRM and RPI records also relate to the possible effect of lock-in delay, which is determined by the sediment depth in which magnetic particles are aligned and 'locked' in the direction of the geomagnetic field during deposition and cannot be realigned during burial (Thompson and Oldfield, 1986). In organic sediments with a low rate of sediment compaction and in cases where biogeochemical processes are the main cause for producing magnetic particles in a sediment column, the lock-in depth might be tens of centimeters, especially under the influence of sediment burrowing or crawling benthic fauna (Roberts and Winklhofer, 2004; Snowball et al., 2013). In sediment records with clastic-biogenic varves, the DRM signal is rapidly locked in the upper few centimeters due to efficient burial and compaction by mineral matter derived from detritus (Snowball et al., 2007; Ojala et al., 2017). Below the uppermost 1 m, the Biển Hồ sediment sequence has a relatively low organic carbon content, a constant water content, a very stable accumulation rate, and expresses fairly small changes in the concentration of detrital material that is carrying the remanence. Combined with an absence of turbidite layers, other indications of suddenly increased accumulation, and bioturbated sections, we consider that the PSV signal in the Biển Hồ sediment sequence is not significantly affected by a paleomagnetic lock-in delay (Nguyễn-Văn et al., 2023) (Supplementary Material S1).

Our chronology builds on 47 ^{14}C samples covering 25 m of core and about 55 ka, which translates to one ^{14}C date every 0.5 m or every 1200 years on average. It is very rare that non-annually laminated lake sediment records have been ^{14}C-dated with higher resolution, and that independent dating methods supplement each other so well. 18 out of these 47 ^{14}C samples are based on bulk organic carbon and are thus potentially prone to a reservoir effect caused by the incorporation of older (dead) carbon. As Biển Hồ is a volcanic maar lake and not located in a carbonate-rich limestone environment, and as the hydrological catchment is relatively limited without long-distance river transport of old, re-worked organic material, any reservoir effect is relatively low and negligible. The two pairs of ^{14}C samples (leaf versus bulk organic carbon) suggest that the incorporation of older, ^{14}C-depleted carbon in the bulk organic carbon samples is in the range of 0.1–1.1 pmC, which translates into age offsets within the range of the 2-σ radiocarbon dating uncertainty.

This comprehensive chronology justifies the presentation of DRM inclination and RPI results in relation to the Bayesian radiocarbon age-depth model (Fig. 13). The curves' distinguished features of inclination and RPI changes since about 55 ka cal BP with high temporal resolution potentially provide valuable reference information for local to regional paleomagnetic correlation. The chronological accuracy of the PSV curves is limited by intrinsic uncertainties of radiocarbon age-depth modeling.

Taken together, the Biển Hồ PSV and RPI curves demonstrate good consistency between reference curves, within a margin of their chronological error estimates. Although chronologies of most individual

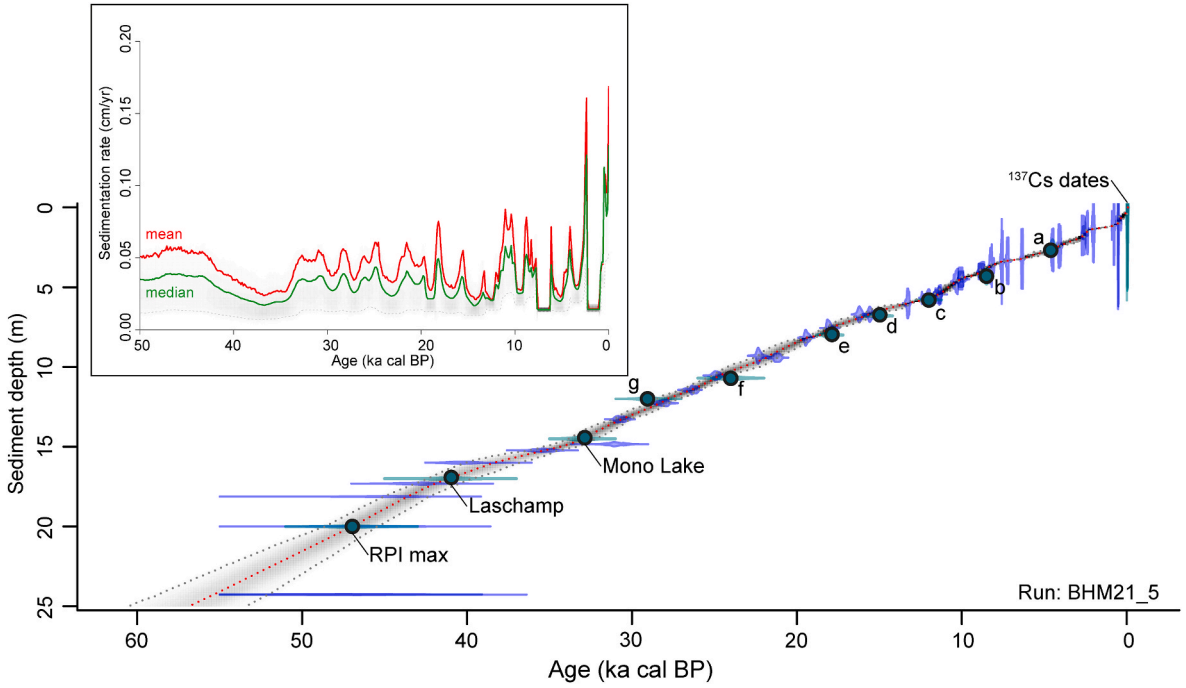

Fig. 12. Bayesian age-depth model of the Biển Hồ maar lake sedimentary sequence with ^{137}Cs and ten paleomagnetic anchor points (●; see details in Fig. 11, Table 3) added, created with the R package *rbacon*. The red dashed line represents the weighted mean; gray dashed lines represent minimum and maximum ranges (95% confidence interval). Blue tie bars indicate the ^{14}C age distribution.

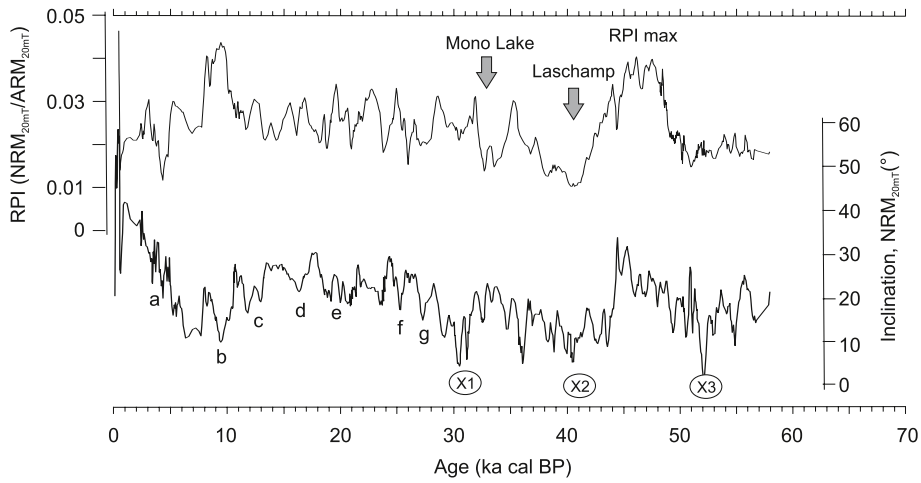

Fig. 13. DRM inclination and RPI variability curves of the Biển Hồ sequence plotted using calibrated radiocarbon ages of the Bayesian age-depth model composed of 47 radiocarbon dates. X1, X2, and X3 represent broad inclination minima that occurred during the Mono Lake – Laschamp interval (~28–45 ka cal BP) (Korte et al., 2019) and at around 50–55 ka cal BP. Details to letters 'a' to 'g' are given in Fig. 9.

reference curves (Ohno et al., 1993; Li et al., 1999; Yamazaki et al., 2003; Ali et al., 1999; Hayashida et al., 2007; Sheng et al., 2019) are based on radiocarbon dating and identification of tephra layers, the dating accuracy of GLOPIS-75 stacked record of geomagnetic paleointensity was confirmed through its correlation to the GISP2 ice core oxygen isotope record (Voelker et al., 1997; Laj et al., 2004). The agreement between the present RPI results and GLOPIS-75 characteristics enhance the reliability of the Biển Hồ paleomagnetic chronology. Finally, we note that the 25-m-deep piston core from 2021 did not reached bedrock, which opens the expectation of extending this valuable sedimentary record far deeper through the ice ages and possibly beyond. Beyond the technical limits of radiocarbon dating, paleomagnetic dating will be essential for establishing the chronology of deeper cores from the future coring campaigns that can potentially tie into Norwegian-Greenland Sea (64.5 ka BP) and even Blake (116.5 ± 0.7 ka BP and 112.0 ± 1.9 ka BP) excursions (Thompson and Oldfield, 1986; Jacobs, 1994; Korte et al., 2019).

6. Conclusions

Our multi-method sediment chronology for the Biển Hồ 25-m-long sediment sequence extending back to 55 ka cal BP and the related paleomagnetic proxy-record is the longest and most consolidated of its kind in Vietnam and the wider region. Based on age-depth and sediment facies characteristics, we can affirm continuity of sedimentation in the deepest part of Biển Hồ maar lake since 55 ka cal BP and suggest that the sediment sequence represents a complete and uninterrupted record of the lake's depositional history. The benefit of a high-resolution and independently dated age-depth model, forms a solid basis for future studies of paleoclimate and paleoenvironmental changes, particularly targeted to the variability of the East-Asian monsoon system on different timescales. We anticipate that the Biển Hồ sequence will provide enhanced detection and dating of East-Asian tephra, some of which we already identified visually in the lithofacies profile. The present chronology will provide an essential basis in future tephra studies, both for further identification and characterization of known tephra (see Supplementary Material S1), and for the dating of newly recognized tephra.

Declaration of competing interest

The authors declare that they have no known competing financial interests or personal relationships that could have appeared to influence the work reported in this paper.

Data availability

Data will be made available on request.

Acknowledgements

The content of this manuscript is based upon work supported by the Vietnam National Foundation for Science and Technology Development (NAFOSTED) grant number 105.99-2018.316 (H.N.). The manuscript benefited from H.N.'s Fulbright Visiting Scholars Program at the Indiana University in 2021 and NSF-supported training at the LacCore/CSD Facility at the University of Minnesota in 2017, as well as continuing analytical support from LacCore. We are indebted to Jan P. Schimmelmann, Kelsey E. Doiron, Nguyễn T. Hồng, Nguyễn T. Dương, Phan T. Tùng, Đặng X. Tùng, Đào T. Hoàn, Nùng V. Minh, and Nguyễn T. A. Nguyệt for assistance during fieldwork and in the laboratory. This article is dedicated to the memory of our colleague Phan T. Tùng who passed away.

Appendix A. Supplementary data

Supplementary data to this article can be found online at https://doi.org/10.1016/j.quageo.2023.101443.

References

Ali, M., Oda, H., Hayashida, A., Takemura, K., Torii, M., 1999. Holocene paleomagnetic secular variation at Lake Biwa, central Japan. Geophys. J. Int. 136, 218–228. https://doi.org/10.1046/j.1365-246X.1999.00718.x.

Appleby, P.G., 2000. Radiometric dating of sediment records in European mountain lakes. J. Limnol. 59, 1–14. https://doi.org/10.4081/jlimnol.2000.s1.1.

Appleby, P.G., 2008. Three decades of dating recent sediments by fallout nuclides: a review. Holocene 18, 83–93. https://doi.org/10.1177/0959683607085598.

Bai, Z.G., Wan, G.J., Huang, R.G., Liu, T.S., 2002. A comparison on the accumulation characteristics of ^{7}Be and ^{137}Cs in lake sediments and surface soils in western Yunnan and central Guizhou, China. Catena 49, 253–270. https://doi.org/10.1016/S0341-8162(02)00004-8.

Blaauw, M., 2010. Methods and code for 'classical' age-modelling of radiocarbon sequences. Quat. Geochronol. 5, 512–518. https://doi.org/10.1016/j.quageo.2010.01.002.

Blaauw, M., Christen, J.A., 2011. Flexible paleoclimate age-depth models using an autoregressive gamma process. Bayesian Anal 6, 457–474. https://doi.org/10.1214/11-BA618.

Blaauw, M., Christen, J.A., Bennett, K.D., Reimer, P.J., 2018. Double the dates and go for Bayes—impacts of model choice, dating density and quality on chronologies. Quat. Sci. Rev. 188, 58–66. https://doi.org/10.1016/j.quascirev.2018.03.032.

Bronk Ramsey, C., 2009. Bayesian analysis of radiocarbon dates. Radiocarbon 51, 337–360. https://doi.org/10.1017/S0033822200033865.

Brown, M., Korte, M., Holme, R., Wardinski, I., Gunnarson, S., 2018. Earth's magnetic field is probably not reversing. Proc. Natl. Acad. Sci. U.S.A. 115, 5111–5116. https://doi.org/10.1073/pnas.1722110115.

Buckley, B.M., Fletcher, R., Wang, S.-Y.S., Zottoli, B., Pottier, C., 2014. Monsoon extremes and society over the past millennium on mainland Southeast Asia. Quat. Sci. Rev. 95, 1–19. https://doi.org/10.1016/j.quascirev.2014.04.022.

Foucher, A., Chaboche, P.-A., Sabatier, P., Evrard, O., 2021. A worldwide meta-analysis (1977–2020) of sediment core dating using fallout radionuclides including ^{137}Cs and ^{210}Pb$_{xs}$. Earth Syst. Sci. Data 13, 4951–4966. https://doi.org/10.5194/essd-13-4951-2021.

Graven, H.D., 2015. Impact of fossil fuel emissions on atmospheric radiocarbon and various applications of radiocarbon over this century. Proc. Natl. Acad. Sci. U.S.A. 112, 9542–9545. https://doi.org/10.1073/pnas.1504467112.

Håkanson, L., Jansson, M., 1983. Principles of Lake Sedimentology. Springer-Verlag, Berlin, p. 316.

Hayashida, A., Ali, M., Kuniko, Y., Kitagawa, H., Torii, M., Takemura, K., 2007. Environmental magnetic record and paleosecular variation data for the last 40 kyrs from the Lake Biwa sediments, Central Japan. Earth Planets Space 59, 807–814. https://doi.org/10.1186/BF03352743.

Ho, H.H., Swennen, R., Cappuyns, V., Vassilieva, E., Neyens, G., Rajabali, M., Tran, T.V., 2013. Assessment on pollution by heavy metals and arsenic based on surficial and core sediments in the Cam River mouth, Haiphong Province, Vietnam. Soil Sediment Contam. Int. J. 22, 415–432. https://doi.org/10.1080/15320383.2013.733445.

Jacobs, J.A., 1994. Reversals of the Earth's Magnetic Field, second ed. Cambridge University Press, p. 346. https://doi.org/10.1017/CBO9780511524929.

Jones, K.B., Hodgins, G.W.L., Dettman, D.L., Andrus, C.F.T., Nelson, A., Etayo-Cadavid, M.F., 2007. Seasonal variations in Peruvian marine reservoir age from pre-bomb Argopecten purpuratus shell carbonate. Radiocarbon 49, 877–888. https://doi.org/10.1017/S0033822200042740.

Kanai, Y., Saito, Y., Tamura, T., Nguyen, V.L., Oanh, T.T.K., Sato, A., 2013. Sediment erosion revealed by study of Cs isotopes derived from the Fukushima Dai-ichi nuclear power plant accident. Geochem. J. 47, 79–82. https://doi.org/10.2343/geochemj.2.0234.

King, J., Banerjee, S.K., Marvin, J., Özdemir, Ö., 1982. A comparison of different magnetic methods for determining the relative grain size of magnetite in natural materials: some results from lake sediments. Earth Planet Sci. Lett. 59, 404–419. https://doi.org/10.1016/0012-821X(82)90142-X.

Klaminder, J., Appleby, P., Crook, P., Renberg, I., 2012. Post-deposition diffusion of 137Cs in lake sediment: implications for radiocaesium dating. Sedimentology 59, 2259–2267. https://doi.org/10.1111/j.1365-3091.2012.01343.x.

Korte, M., Brown, M.C., Panovska, S., Wardinski, I., 2019. Robust characteristics of the Laschamp and Mono Lake geomagnetic excursions: results from global field models. Front. Earth Sci. 7, 86. https://doi.org/10.3389/feart.2019.00086.

Laj, C., Kissel, C., Mazaud, A., Channel, J.E.T., Beer, J., 2000. North Atlantic paleointensity stack since 75 ka (NAPIS-75) and the duration of the Laschamp event. Phil. Trans. Royal Soc. A 358, 1009–1025. https://doi.org/10.1098/rsta.2000.0571.

Laj, C., Kissel, C., Beer, J., 2004. High resolution global paleointensity stack since 75 kyr (GLOPIS-75) calibrated to absolute values. Geophys. Monogr. 145, 255–265. https://doi.org/10.1029/145GM19.

Levi, S., Banerjee, S.K., 1976. On the possibility of obtaining relative paleointensities from lake sediments. Earth Planet Sci. Lett. 29, 219–226. https://doi.org/10.1016/0012-821X(76)90042-X.

Li, P., Wang, Y., Liu, Z., 1999. Chronostratigraphy of chongsheng Sea and its sedimentary rate. Sci. China, Ser. A D 29, 50–55 (in Chinese).

Liu, J., Nowaczyk, N.R., Panovska, S., Korte, M., Arz, H.W., 2020. The Norwegian-Greenland Sea, the Laschamps, and the Mono Lake excursions recorded in a Black Sea sedimentary sequence spanning from 68.9 to 14.5 ka. J. Geophys. Res. Solid Earth 125, e2019JB019225. https://doi.org/10.1029/2019JB019225.

Long, N.Q., Truong, Y., Hien, P.D., Binh, N.T., Sieu, L.N., Giap, T.V., Phan, N.T., 2012. Atmospheric radionuclides from the Fukushima Dai-ichi nuclear reactor accident observed in Vietnam. J. Environ. Radioact. 111, 53–58. https://doi.org/10.1016/j.jenvrad.2011.11.018.

Lowe, D.J., 2011. Tephrochronology and its application: a review. Quat. Geochronol. 6, 107–153. https://doi.org/10.1016/j.quageo.2010.08.003.

Lu, X., 2004. Application of the weibull extrapolation to 137Cs geochronology in tokyo bay and ise bay, Japan. J. Environ. Radioact. 73, 169–181. https://doi.org/10.1016/j.jenvrad.2003.08.009.

Mankinen, E.A., Wenthworth, C.M., 2004. Mono Lake excursion recorded in sediment of the santa clara valley, California. G-cubed 5, Q02H05. https://doi.org/10.1029/2003GC000592.

Muscheler, R., Adolphi, F., Svensson, A., 2014. Challenges in 14C dating towards the limit of the method inferred from anchoring a floating tree ring radiocarbon chronology to ice core records around the Laschamp geomagnetic field minimum. Earth Planet Sci. Lett. 394, 209–215. https://doi.org/10.1016/j.epsl.2014.03.024.

Nguyễn, H., Flower, M.F.J., Cung, T.C., Phạm, T.X., Hoàng, V.Q., Trần, T.S., 2013. Collision-induced basalt eruptions at Pleiku and buôn mê thuột, south-central Vietnam. J. Geodyn. 69, 65–83. https://doi.org/10.1016/j.jog.2012.03.012.

Nguyễn-Đình, T., Nguyễn-Thùy, D., Nguyễn-Văn, H., Ojala, A.E.K., Sauer, P.E., Schimmelmann, A., Unkel, I., 2022. High-resolution, 1250-year long drought record from ea tyn lake, central Highlands of việt nam. Holocene 32, 1026–1040. https://doi.org/10.1177/09596836221106967.

Nguyễn-Khắc, S., 2007. Prehistoric Archaeology in the Central Highlands. Education Publishing House, Hanoi, p. 277 (in Vietnamese).

Nguyễn-Văn, H., Schimmelmann, J.P., Nguyễn-Thùy, D., Ojala, A.E.K., Unkel, I., Nguyễn-Đình, T., Fukumoto, Y., Doiron, K.E., Sauer, P.E., Drobniak, A., Nguyễn-Thùy, D., Nguyễn, T.A.N., Đỗ-Trọng, Q., Nguyễn-Thị, H., Nguyễn-Ánh, D., Nguyễn-Văn, T., Schimmelmann, A., 2022. Environmental history recorded over the last 70 years in Biển Hồ maar sediment, central Highlands of Vietnam. Quat. Int. 621, 84–100. https://doi.org/10.1016/j.quaint.2020.05.013.

Nguyễn-Văn, H., Unkel, I., Nguyễn-Thùy, D., Nguyễn-Đình, Trọng Quốc, Đ., Xuân Tùng, Đ., Thị Hồng, N., Xuân Thành, Đ., Thị Ánh Nguyệt, N., Hồng Quân, N., Trung Hoàn, Đ., Thị Huyền Trang, N., Lê Tuyết Nhung, P., Nguyệt Anh, L., Văn Hà, V., Ojala, A.E.K., Schimmelmann, A., Sauer, P., 2023. Paleoenvironmental potential of lacustrine sediments in the Central Highlands of Vietnam: a review on the state of research. Vietnam Journal of Earth Sciences. https://doi.org/10.15625/2615-9783/18281 (in press).

Nowaczyk, N.R., Frank, U., Kind, J., Arz, H.W., 2013. A high-resolution paleointensity stack of the past 14 to 68 ka from Black Sea sediments. Earth Planet Sci. Lett. 384, 1–16. https://doi.org/10.1016/j.epsl.2013.09.028.

Ochiai, S., Nagao, S., Yamamoto, M., Itono, T., Kashiwaya, K., Fukui, K., Iida, H., 2013. Deposition records in lake sediments in western Japan of radioactive Cs from the Fukushima Dai-ichi nuclear power plant accident. Appl. Radiat. Isot. 81, 366–370. https://doi.org/10.1016/j.apradiso.2013.03.073.

Ohno, M., Hamano, Y., Murayama, M., Matsumoto, E., Iwakura, H., Nakamura, T., Taira, A., 1993. Paleomagnetic record over the past 35,000 years of a sediment core from off Shikoku, Southwest Japan. Geophys. Res. Lett. 20, 1395–1398. https://doi.org/10.1029/93GL01241.

Ojala, A.E.K., Luoto, T.P., Virtasalo, J.J., 2017. Establishing a high-resolution surface sediment chronology with multiple dating methods - testing ^{137}Cs determination with Nurmijärvi clastic-biogenic varves. Quat. Geochronol. 37, 32–41. https://doi.org/10.1016/j.quageo.2016.10.005.

Reimer, P., Austin, W., Bard, E., Bayliss, A., Blackwell, P., Bronk Ramsey, C., Butzin, M., Cheng Edwards, L.R., Friedrich, M., Grootes, P.M., Guilderson, T.P., Hajdas, I., Heaton, T.J., Hogg, A.G., Hughen, K.A., Kromer, B., Manning, S.W., Muscheler, R., Palmer, J.G., Pearson, C., van der Plicht, J., Reimer, R.W., Richards, D.A., Scott, E. M., Southon, J.R., Turney, C.S.M., Wacker, L., Adolphi, F., Büntgen, U., Capano, M., Fahrni, S.M., Fogtmann-Schulz, A., Friedrich, R., Köhler, P., Kudsk, S., Miyake, F., Olsen, J., Reinig, F., Sakamoto, M., Sookdeo, A., Talamo, S., 2020. The IntCal20 Northern Hemisphere radiocarbon age calibration curve (0-55 cal kBP). Radiocarbon 62 (4), 725–757. https://doi.org/10.1017/RDC.2020.41.

Roberts, A.P., Winklhofer, M., 2004. Why are geomagnetic excursions not always recorded in sediments? Constraints from post-depositional remanent magnetization lock-in modelling. Earth Planet Sci. Lett. 227, 345–359. https://doi.org/10.1016/j.epsl.2004.07.040.

Sheng, M., Wang, X., Dekkers, M.J., Chen, Y., Chu, G., Tang, L., Pei, J., Yang, Z., 2019. Paleomagnetic Secular variation and Rrlative paleointensity during the Holocene in South China-Huguangyan maar lake revisited. G-cubed 20, 2681–2697. https://doi.org/10.1029/2018GC008106.

Slota, P.J., Jull, A.J.T., Linick, T.W., Toolin, L.J., 1987. Preparation of small samples for ^{14}C accelerator targets by catalytic reduction of CO. Radiocarbon 29, 303–306. https://doi.org/10.1017/S0033822200056988.

Smol, J.P., 2008. Pollution of Lakes and Rivers: A Paleoenvironmental Perspective, second ed. Blackwell Publishing Ltd, Oxford, p. 383.

Snowball, I., Zillén, L., Ojala, A., Saarinen, T., Sandgren, P., 2007. FENNOSTACK and FENNORPIS: varve dated Holocene palaeomagnetic secular variation and relative palaeointensity stacks for Fennoscandia. Earth Planet Sci. Lett. 255, 106–116. https://doi.org/10.1016/j.epsl.2006.12.009.

Snowball, I., Mellström, A., Ahlstrand, E., Haltia, E., Nilsson, A., Ning, W., Muscheler, R., Brauer, A., 2013. An estimate of post-depositional remanent magnetization lock-in depth in organic rich varved lake sediments. Global Planet. Change 110, 264–277. https://doi.org/10.1016/j.gloplacha.2013.10.005, 2013.

Tauxe, L., 1993. Sedimentary records of relative paleointensity of geomagnetic field: theory and practice. Rev. Geophys. 31, 319–354. https://doi.org/10.1029/93RG01771.

Thompson, R., 1986. Modelling magnetization data using SIMPLEX. Phys. Earth Planet. In. 42, 113–127. https://doi.org/10.1016/S0031-9201(86)80013-9.

Thompson, R., Oldfield, F., 1986. Environmental Magnetism. Allen & Unwin, London, p. 227. https://doi.org/10.1007/978-94-011-8036-8.

Tivey, M., Johnson, H.P., 1981. Characterization of viscous remanent magnetization in single- and multi-domain magnetite grains. Geophys. Res. Lett. 8, 217–220. https://doi.org/10.1029/GL008i003p00217.

Voelker, A., Sarnthein, M., Grootes, P., Erlenkeuser, H., Laj, C., Mazaud, A., Nadeau, M.-J., Schleicher, M., 1997. Correlation of marine 14C ages from the Nordic Seas with the GISP2 isotope record: implications for 14C calibration beyond 25 ka BP. Radiocarbon 40, 517–534. https://doi.org/10.1017/S0033822200018397.

Wright, S.M., Howard, B.J., Strand, P., Nylen, T., Sickel, M.A.K., 1999. Prediction of ^{137}Cs deposition from atmospheric nuclear weapons tests within the Arctic. Environ. Pollut. 104, 131–143. https://doi.org/10.1016/S0269-7491(98)00140-7.

Yamazaki, T., Abdeldayem, A.L., Ikehara, K., 2003. Rock-magnetic changes with reduction diagenesis in Japan Sea sediments and preservation of geomagnetic secular variation in inclination during the last 30,000 years. Earth Planets Space 55, 327–340. https://doi.org/10.1186/BF03351766.

Yang, Z., Heller, F., Wu, N., Jie, Y., Zhihua, S., 2009. Geomagnetic paleointensity dating of South China Sea sediments for the last 130 kyr. Earth Planet Sci. Lett. 284, 258–266. https://doi.org/10.1016/j.epsl.2009.04.035.

Zolitschka, B., Francus, P., Ojala, A.E.K., Schimmelmann, A., 2015. Varves in lake sediments – a review. Quat. Sci. Rev. 117, 1–41. https://doi.org/10.1016/j.quascirev.2015.03.019.